ARTICLE

ACS chemical biology

An Integrated-Molecule-Format Multicolor Probe for Monitoring Multiple Activities of a Bioactive Small Molecule

Sung Bae Kim[†], Yoshio Umezawa[‡], Kira A. Kanno[‡], and Hiroaki Tao[†,*]

[†]Research Institute for Environmental Management Technology, National Institute of Advanced Industrial Science and Technology (AIST), 16-1 Onogawa, Tsukuba 305-8569, Japan and [‡]Department of Chemistry, School of Science, The University of Tokyo, 7-3-1 Hongo, Bunkyo-Ku, Tokyo 113-0033, Japan

ABSTRACT Bioactive small molecules, including steroids, activate multiple signaling pathways in mammalian cells. However, current technologies cannot illuminate such multiple effects of a ligand in mammalian cells. Here, we demonstrate integrated-molecule-format multicolor systems simultaneously visualizing bifacial activities of a ligand, where estrogen receptor α (ERα) was exemplified to demonstrate the present technology. First, we developed a single-molecule-format probe emitting red bioluminescence for imaging interaction between the phosphorylated ligand binding domain of ERα (ER LBD) and the Src homology-2 (SH2) domain of Src. The SH2 domain-linked ER LBD was sandwiched between dissected N- and C-terminal fragments of *Pyrophorus plagiophthalamus* (click beetle) luciferase emitting red bioluminescence. Second, another single-molecule-format bioluminescent probe emitting green bioluminescence was constructed to visualize intramolecular interaction between ER LBD and LXXLL motifs. Mammalian cells carrying the two probes emit red and/or green light in response to agonistic and antagonistic activities of a ligand, which correspond to its genomic and nongenomic activities, respectively. Third, the two probes were assembled to make an single-molecule-format multicolor indicator, in which all of the components for ligand sensing and multiple-light emission were integrated. The probe emitted characteristic light spectra in response to various agonists and antagonists. This is the first example where (i) protein phosphorylation was recognized with a single bioluminescent probe and (ii) bifacial activities of a ligand, either agonistic or antagonistic, were simultaneously visualized with multiple colors.

An agonist is defined as a substance that binds to a specific receptor and triggers a response in the cells. However, it sometimes acts in opposite roles unexpectedly, like a "double-edged sword" (*1*). A recent study also revealed an example that steroids simultaneously stimulate both genomic and nongenomic signaling pathways through the androgen receptor in mammalian cells, whereas some chemicals activate only one of the pathways (*2*). A crosstalk between distinct signaling pathways also makes ligand-activated signalings complicated in living cells. These previous studies strongly suggest that the roles of a ligand are much more complex and multifacial than ever expected in the physiological circumstances of living cells. Thus, it is rational to simultaneously determine such multiple, occasionally bifacial activities of a ligand in living cells to understand the ligand actions. However, such multistimulative, bifacial activities of a ligand for various signaling pathways are hard to estimate, owing to the lack of a suitable methodology.

Recent studies have invented various bioanalytical technologies with reporter proteins that determine ligand activities on the basis of protein−protein interactions in living subjects (*3, 4*). Reporter proteins with optical signatures, either fluorescent or bioluminescent, are excellent functional materials for real-time analysis of ligand activities in cells or in small animal models (*4–9*).

Reporter proteins emitting bioluminescence have been used to examine ligand activities (*2–4, 6, 10, 11*). The luciferases are categorized into two groups: pH-sensitive and pH-insensitive (*5*). *Pyrophorus plagiophthalamus* (click beetle) luciferase (CB) is less sensitive to pH, temperature, and heavy metal ions and is

*Corresponding author, hiro-tao@aist.go.jp.

Received for review January 6, 2008 and accepted May 21, 2008.

Published online June 20, 2008

10.1021/cb800004s CCC: $40.75

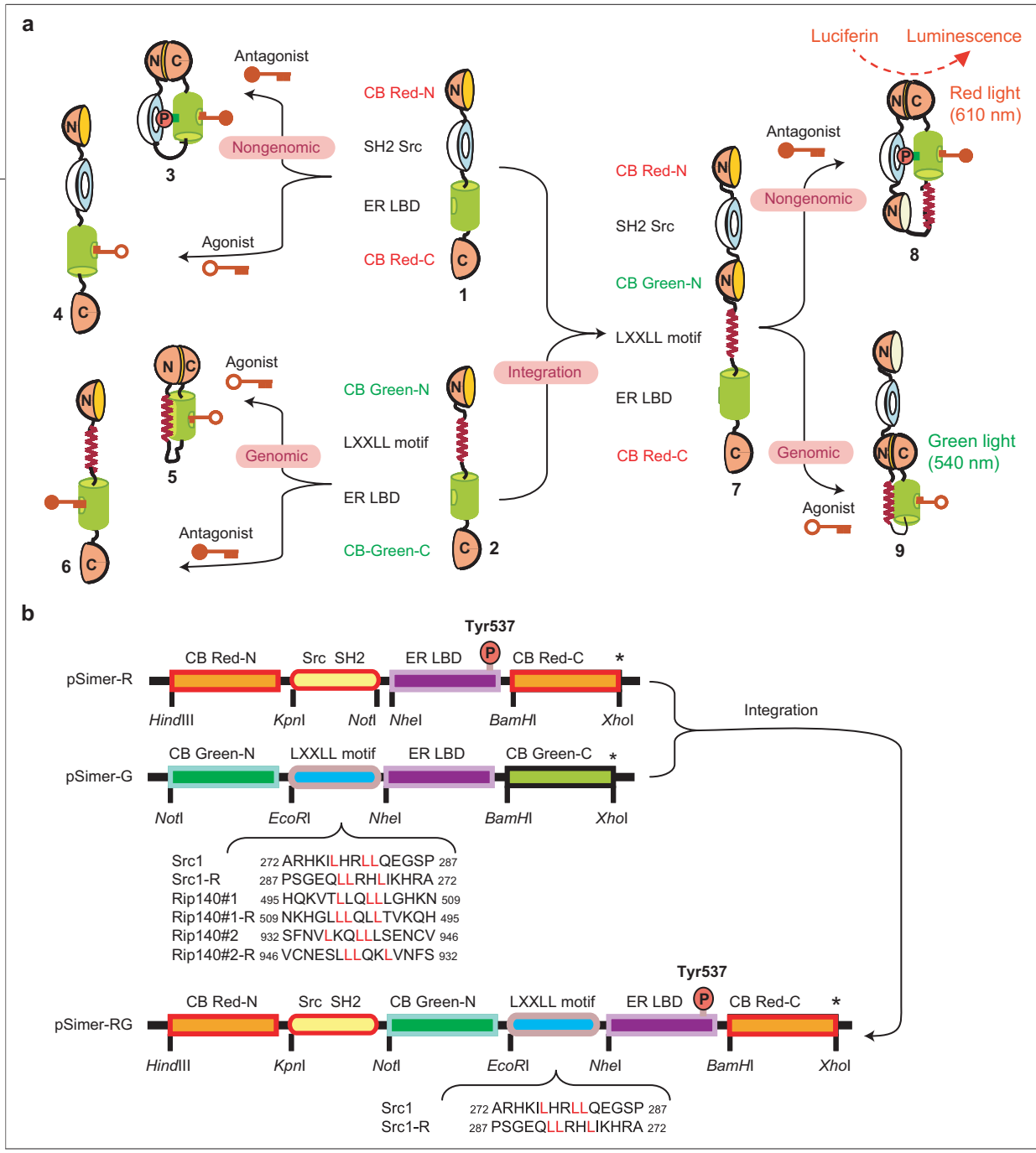

Figure 1. a) Schematic illustration showing the ligand-sensing mechanism of probes. Structures 1, 2, and 7 show the probe structures expressed from pSimer-R and pSimer-G series plasmids or pSimer-RG series plasmids, respectively. Structures 3 and 4 indicate the molecular structures of pSimer-G series probes stimulated with agonist and antagonist, respectively. On the other hand, structures 5 and 6 represent pSimer-G series probes upon being stimulated with agonist or antagonist. The core domains of pSimer-R and -G series plasmids were assembled in a single construct, in which all of the components for ligand sensing and multiple color development were integrated, shown with structure 7. The expected molecular structures with agonist and antagonist are illustrated in structures 8 and 9, respectively. Abbreviations: Src SH2, SH2 domain of Src; ER LBD, ligand-binding domain of estrogen receptor; CB Red-N, N-terminal domain of click beetle luciferase red; CB Green-C, C-terminal domain of click beetle luciferase green. b) Schematic diagrams of cDNA constructs. The component cDNA domains of each plasmid were specified. The present series of plasmids were named "pSimer," which means a plasmid encoding a Simer.

thus an optimal reporter protein for visualizing a ligand activity of interest inside living subjects. These split reporter proteins have been used for measuring biologically meaningful protein–protein interactions inside cells or living animals, where the activity of the reporter proteins is temporarily lost by splitting and recovered by protein complementation or protein splicing (*3, 10*). These bioanalytical systems typically comprise two component plasmids. They should be cotransfected and equally expressed in a cell for optimum efficiency.

Very recently, we validated a smart single-molecule-format bioluminescent probe for determining protein−protein or protein−peptide interactions (*11, 12*). The probe contains N- and C-terminal fragments of a split *Photinus pyralis* (firefly) luciferase (FLuc), between which two proteins of interest were inserted. The probe is characterized as a single-molecule-format bioluminescent indicator, in which all of the components required for signal sensing and light emission are integrated. Despite the recent, intensive studies, all of the conventional methods do not provide a simultaneous determination of multiple, bifacial activities of a ligand in living cells.

Estrogen receptor (ER) is a member of the steroid hormone receptor superfamily of ligand-activated transcription factors (*13, 14*). Estrogens exert their effects through the actions of ERs such as dimerization and coactivator recruitment for gene expression (genomic actions). However, a number of other effects of estrogens such as kinase activation in the cytosol are so rapid that they cannot be related with direct gene expression. These actions are known as nongenomic actions and are mediated through membrane-associated ERs (*14*). Here, we represent a new bioanalytical method with single-molecule-format multicolor probes for simultaneous determination of multiple effects of a ligand. These probes were named "Simer" (single molecule-format multicolor probe with estrogen receptor), and the assay can be called a Simer assay.

First, we constructed a single-molecule-format probe emitting red light for determining tyrosine phosphorylation of the ligand-binding domain of ER (ER LBD). The phosphorylation of ER at tyr537 is mediated by cytoplasmic Src (*15*) and thus can be an index for nongenomic actions of ER mediated by Src. ER LBD was connected to the phosphorylation recognition domain (Src homology-2 (SH2) domain) of a proto-oncogene tyrosine-protein kinase, Src, through a flexible GS linker and then sandwiched between the dissected N- and C-terminal fragments of CB emitting red light (CB Red). Upon stimulation with an antagonist, the ER LBD inside the probe interacts with its counterpart Src SH2, and the subsequent intramolecular complementation between the respective N- and C-terminal fragments triggers the recovery of the luciferase activities emitting red light (Figure 1, panel a).

Second, another single-molecule-format probe emitting green light was made for estimating the binding of ER LBD with an LXXLL motif of coactivators as an index for genomic activities of ligands. ER LBD binds to an α-helical LXXLL motif of coactivators in a ligand-dependent manor in the genomic pathway, where the motif is necessary and sufficient to mediate the ligand-dependent binding (*16, 17*). For this probe, ER LBD was fused with an LXXLL motif, both ends of which were connected with, respectively, N- and C-terminal fragments of CB emitting green light (CB Green). The luciferase activity of the fragmented CB Green inside the probes is designed to be temporarily lost. Upon stimulation with an agonist, the ER LBD inside the probe interacts with its counterpart peptide, and subsequently the activities of CB Green are recovered through the complementation between the N- and C-terminal fragments.

The plasmid set with the probes emitting red and green light was then transfected into COS-7 cells for the simultaneous estimation of agonistic and antagonistic activities of a ligand with colors. The green and red lights in response to agonistic and antagonistic activities of a ligand correspond respectively to their genomic activities and nongenomic activities mediated by Src.

In addition, the key elements of the two red- and green-light-emitting probes were integrated in a single molecule for making a multicolor probe ligand-dependently emitting red and/or green light, which corresponds to bifacial effects of a ligand. The COS-7 cells carrying the single-molecule-format multicolor probe, SIMER-RG2, exhibited characteristic fingerprint spectra in response to agonists and antagonists. SIMER-RG2 is a single molecule, and thus its spectrum is not influenced by the individual expression variances in every batch. In contrast, pSimer-R and -G should be cotransfected for multicolor imaging and thus express diverse levels of indivisual probes in every batch. Their spectra cannot be fingerprints for a ligand. The present integrated-molecule-format multicolor probes provide a high-throughput molecular imaging scheme for illuminating simultaneously multiple activities of a ligand in living mammalian cells.

RESULTS

Development of a Single-Molecule-Format Red Luminescent Probe Reporting Phosphorylations of Ligand-Binding Domain of ERα. We first made a series of single-molecule-format probes, emitting red light, to decide optimal dissection points of CB Red. These probes were designed for imaging ER LBD-Src SH2 inter-

actions via intramolecular complementation of the flanking N- and C-terminal fragments of CBs (see pSimer-R in Figure 1, panel b). The results in Figure 2, panel a(i) show that COS-7 cells carrying pSimer-R2, comprising 1−412 aa and 413−542 aa fragments of CB Red, exhibit the highest luminescence intensities and signal-to-background ratios up to a 5.6-fold increase. The subsequent luminescence spectra show that COS-7 cells carrying pSimer-R2 emitted enhanced red light at 610 nm in the presence of 4-hydroxytamoxifen (OHT) (Figure 2, panel a(iii)).

The selectivity of the fusion protein probe expressed from pSimer-R2 (SIMER-R2) to various ligands was determined in the following mammalian cells (Figure 2, panel b): human cervical epithelioid carcinoma derived HeLa cell, African green monkey kidney derived COS-7 cell, murine embryo fibroblast derived NIH 3T3 cell, and human breast cancer derived MCF-7 cell. The probe exhibited selective recognition for a known estrogen antagonist, OHT or ICI 182780, in any cell lines. On the other hand, it showed a weak or no response to known estrogen agonists including E_2. Epidermal growth factor (EGF), a protein tyrosine kinase activator, did not stimulate the probe from pSimer-R2 (Supplementary Figure 1).

Kinetics of the probe from pSimer-R2 in ligand recognition was monitored on the basis of the emitted luminescence intensities (Figure 2, panel c). OHT triggered a rapid increase in luminescence emission from COS-7 cells carrying pSimer-R2; it was not so with E_2 during the monitored time range, 0−25 min. The luminescence intensities by OHT reached a plateau at 15 min.

The experiments in Figure 2, panels a−c did not provide direct evidence whether phosphorylation of Tyr537 inside ER LBD indeed motivated the intramolecular ER LBD-Src SH2 binding. Therefore, we performed a mutagenesis study to examine the phosphorylation dependence of the binding (Figure 2, panel d). The known ligand-dependent phosphorylation site in ER LBD, Tyr537, was mutated to Phe537, and the mutated plasmid at this point was named pSimer-R2m. This mutagenesis study revealed that COS-7 cells carrying pSimer-R2m are insensitive to both estrogen agonist E_2 and antagonist OHT, whereas COS-7 cells with pSimer-R2 sensed OHT and E_2. The cells with pSimer-R2 exhibited much more enhanced luminescence intensities to OHT (6.3-fold increase) than to E_2 (2-fold increase). In addition, we verified whether OHT and/or E_2 phosphorylate ERα at Y537 with a Western blot analysis (Figure 2, panel e). The results show that anti-Y537 antibody (ERα) recognized specific proteins at ~100 kD in lanes 2 and 3, which are the same as the expected molecular weight of the fusion proteins. On the other hand, the antibody did not blot any specific bands in lanes 4−6. We found that both OHT and E_2 phosphorylate ER at Y537 with a similar extent.

Development of a Single-Molecule-Format Green Luminescent Probe Reporting ER LBD-LXXLL Motif Binding. We first decided on an α-helical LXXLL motif adaptable for a single-molecule-format bioluminescent probe emitting green luminescence (Figure 1, panels a and b). The series of plasmids were named pSimer-G1 to -G6, in which the LXXLL motif sequences differed. In a single fusion protein, ER LBD has two choices to bind a LXXLL motif: parallel or antiparallel orientations. We examined whether the binding nature of ER LBD with LXXLL motifs is parallel or antiparallel by using reverse LXXLL peptides. The sensitivities of each probe to ligands were examined in the presence of 10^{-5} M E_2 or OHT (Figure 3, panel a(i)). COS-7 cells carrying pSimer-G6 exhibited the highest luminescence intensities in response to E_2 and comparably weak luminescence intensities to OHT. The subsequent luminescence spectra exhibited green luminescence with a peak at 540 nm (Figure 3, panel a(iii)).

Dose−response curves for ligands were drawn on the basis of the luminescence intensities from COS-7 cells carrying pSimer-G4 or pSimer-G6. In both cases with pSimer-G4 and -G6, the luminescence intensities were increased in the range of 10^{-8} to 10^{-5} M E_2 (Figure 3, panel b). SIMER-G6 selectively sensed E_2 beyond OHT and emitted stronger luminescence intensities than did the cells with SIMER-G4. The strongest signal feature of SIMER-G6 suggests that ER LBD is likely to bind a LXXLL motif with an antiparallel orientation. This conclusion is consistent with the previous observation based on X-ray crystallography data (Protein Data Bank ID 2J7X).

The reversibility of SIMER-G6 to E_2 was examined by replacing the culture medium with a fresh one (Figure 3, panel b(iii)). COS-7 cells carrying pSimer-G6 stimulated with vehicle (0.1% (v/v) DMSO) did not enhance the luminescence intensities, whereas the cells stimulated with E_2 emitted luminescence intensities 4.3 times stronger than the background. The elevated luminescence intensities were sustained at least for 150 min.

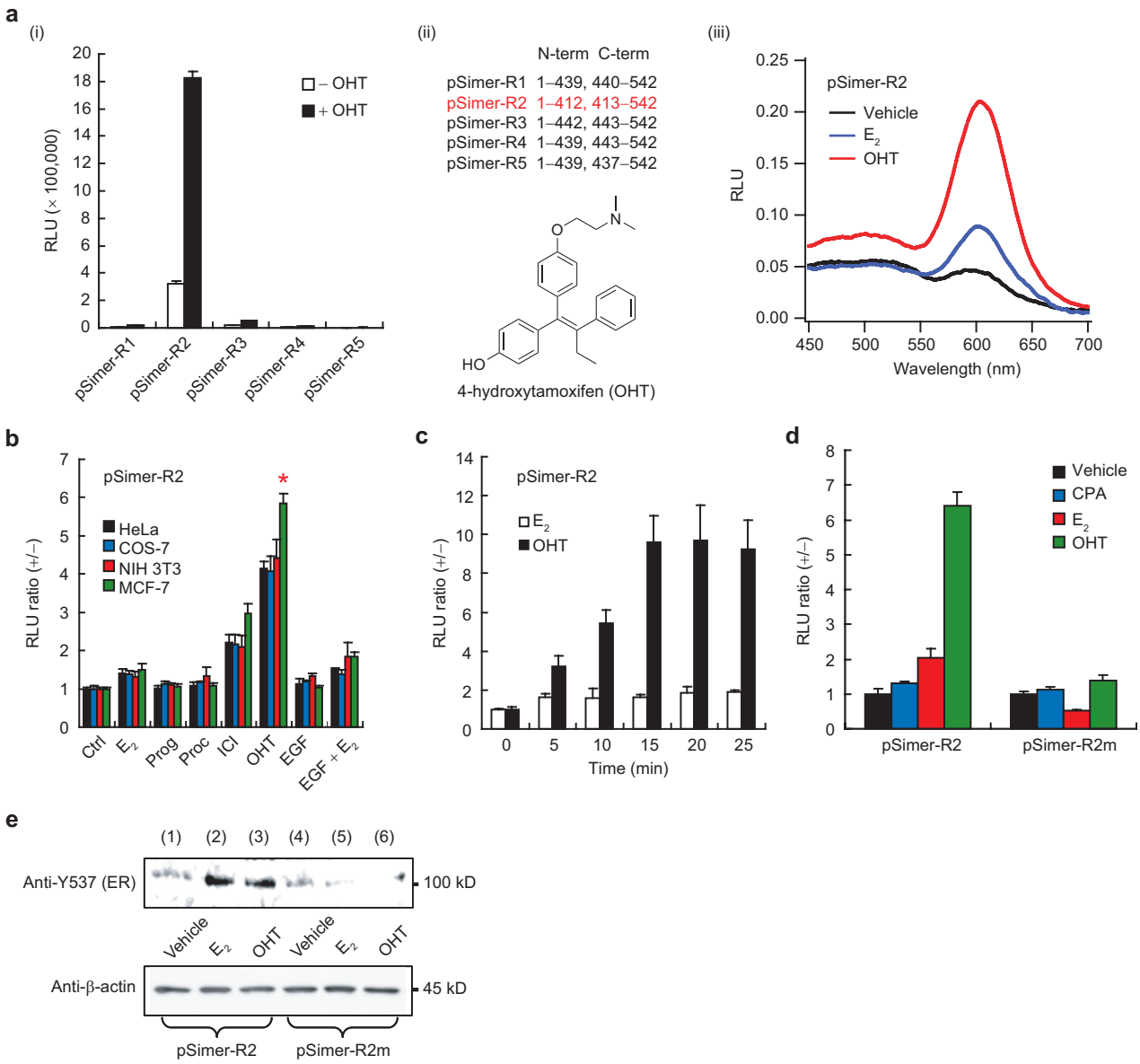

Figure 2. a) Antagonist sensitivity of the probes expressed from pSimer-R1 to -R5. (i) The absolute luminescence intensities by each probe in response to OHT ($n = 3$). (ii) The chemical structure of OHT and the amino acid lengths of N- and C-terminal fragments in each plasmid. (iii) Luminescence spectra for pSimer-R2 in response to vehicle (0.1% v/v DMSO), E_2, or OHT. b) Luminescence intensities of various cell lines carrying pSimer-R2 in response to ligands. Abbreviations: Ctrl, control; E_2, 17β-estradiol; prog, progesterone; proc, procymidone; ICI, ICI 182780; OHT, 4-hydroxytamoxifen; EGF, epidermal growth factor ($n = 3$). c) Ligand-dependent kinetics in the luminescence intensities from COS-7 cells carrying pSimer-R2. The cells were stimulated with E_2 or OHT. The subsequent luminescence intensities were recorded every 5 min ($n = 3$). d) Mutagenesis study for the association of ER LBD with SH2 domain of Src. Tyr537 of ER LBD in pSimer-R2 was replaced with phenylalanine, and the plasmid was named pSimer-R2m. The luminescence intensities from COS-7 cells carrying pSimer-R2 or pSimer-R2m were recorded in response to various ligands ($n = 3$). e) Western blot analysis for determining tyrosine phosphorylation of ER at Y537. Lanes 1–3 show the blots of SIMER-R2, whereas lanes 4–6 are of SIMER-R2m.

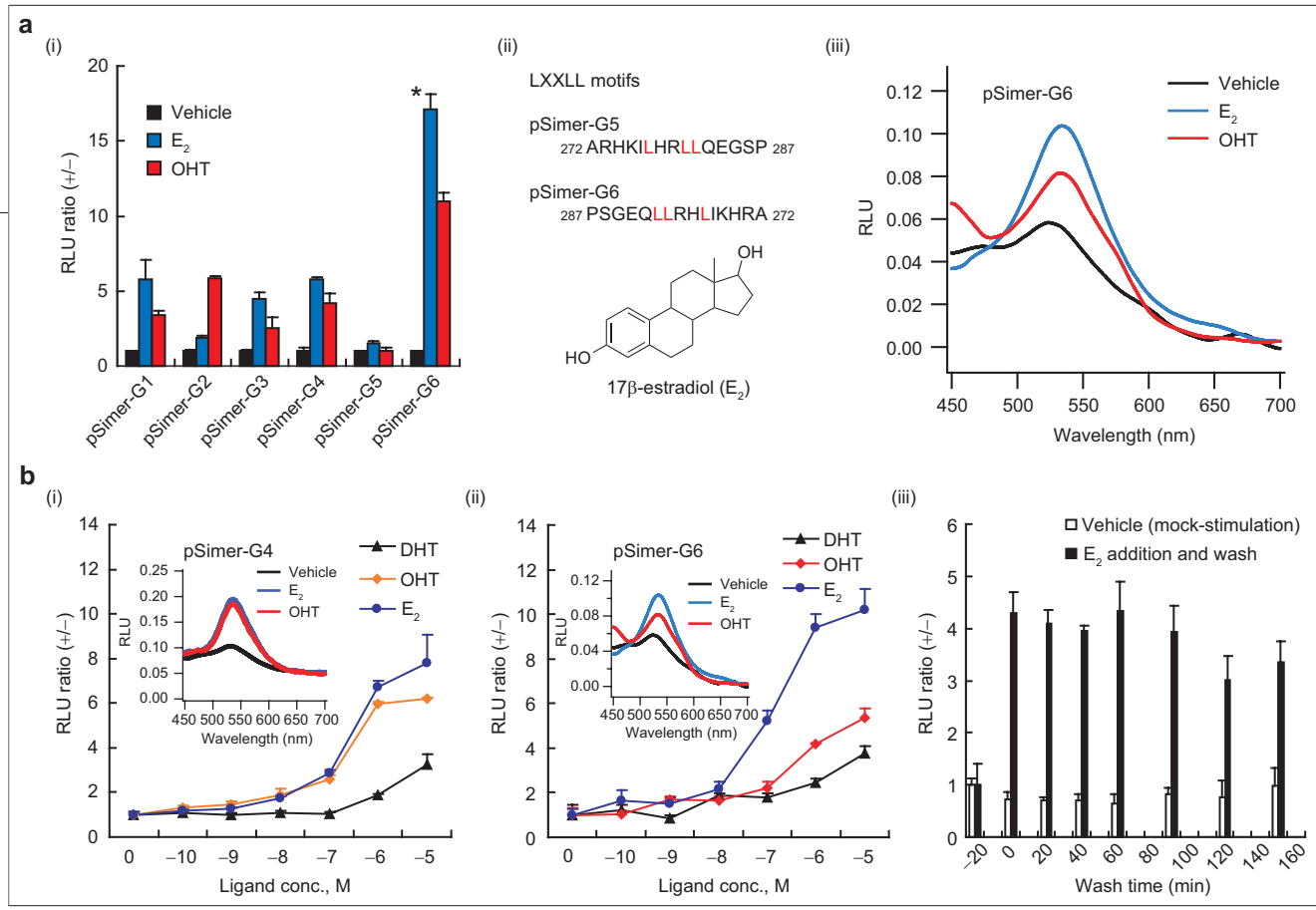

Figure 3. a) Optical property of pSimer-G series probes in response to ligands. (i) Determination of the binding affinity of ER LBD with various LXXLL motifs in response to ER agonist or antagonist ($n = 3$). (ii) LXXLL motif sequences of Src1 (pSimer-G5) and Src1-R (pSimer-G6) (upper). Chemical structure of 17β-estradiol (E_2; lower). (iii) Luminescence spectra of pSimer-G6 in response to ligands. b) Dose—response curves for ligands based on luminescence intensities of COS-7 cells carrying pSimer-G4 (i) or pSimer-G6 (ii). The insets inside panels b(i) and b(ii), respectively, show the luminescence spectra of pSimer-G4 and pSimer-G6 in response to ligands ($n = 3$). (iii) Reversibility of SIMER-G6 after binding E_2. The *x*-axis shows the wash time after medium replacement.

The results show that E_2-bound SIMER-G6 is irreversible even after washing for 150 min.

A mammalian two-hybrid assay was conducted to cross-check LXXLL motif-ER LBD binding (Supplementary Figure 2). Both E_2 and OHT increased the luminescence intensities compared with the control (0.1% (v/v) DMSO). The fold induction ratios show that E_2 is more potent for inducing LXXLL motif-ER LBD binding than OHT, the consequence of which was correspondent to the present result with SIMER-G6.

Simultaneous Determination of Agonistic and Antagonistic Activities of a Ligand with Multicolor from Cells Carrying Multiple Probes. The previous sections showed that pSimer-G and -R series probes were, respectively, green- and red-light-emitting probes in response to ER agonist and antagonist. Here, we examined the color variances emitted from COS-7 cells carrying both pSimer-G4 and pSimer-R2 (Figure 4, panel a). pSimer-G4 was examined here because it induced the largest photon counts and fair signal-to background ratios among the candidates. E_2 enhanced the green color intensity from the cells, whereas OHT increased the red color intensity. Androgens weakly raised both green and red light. We found that known endocrine-disrupting chemicals (EDCs) also weakly facilitated both green and red right.

A total of nine ligands were examined with this method. To normalize the bifacial activities of each ligand, we now suggest an estrogenicity score (ES): $ES = (LI_{540} - IC_{540})/(LI_{610} - IC_{610})$, where LI_{540} and LI_{610} indicate the luminescence intensity at 540 and 610 nm, respectively, upon stimulation with a ligand. On the other hand, IC_{540} and IC_{610} mean the basal (control) intensities at 540 and 610 nm, respectively, upon treatment with a vehicle (0.1% v/v DMSO). The ES of ligands are summarized in Supplementary Table 1.

In addition, we examined the ligand sensitivities of COS-7 cells carrying both pSimer-G6 and pSimer-R2, which were respectively optimal probes for evaluating genomic and nongenomic activities of a ligand in the ER signaling pathway. The color variances of the cells in response to a ligand were shown in Figure 4, panel b. A similar result with Figure 4, panel a was obtained: agonists enhanced the green color intensity, whereas an-

tagonists increased the red color intensities from the cells. Crosstalk agonists and EDCs weakly raised both green and red light. The ES are summarized in Supplementary Table 2.

Simultaneous Determination of Agonistic and Antagonistic Activities of a Ligand with a Single-Molecule-Format Multicolor Probe. Luminescence spectra from COS-7 cells carrying pSimer-RG1 or pSimer-RG2 in response to a ligand were monitored (Figure 5, panel a). COS-7 cells carrying pSimer-RG1 exhibited high background intensities at 540 nm and showed no considerable changes in the spectra in response to E_2 or OHT. On the other hand, COS-7 cells carrying pSimer-RG2 provided a comparably low background luminescence upon stimulation with a vehicle (0.1% v/v DMSO). The bands at 540 and 610 nm were considerably changed in response to E_2 or OHT. pSimer-RG3 comprising an extended GS linker between CB Green-N and LXXLL mofif (20 GS linker) did not exhibit an improved variation of the spectra (data not shown).

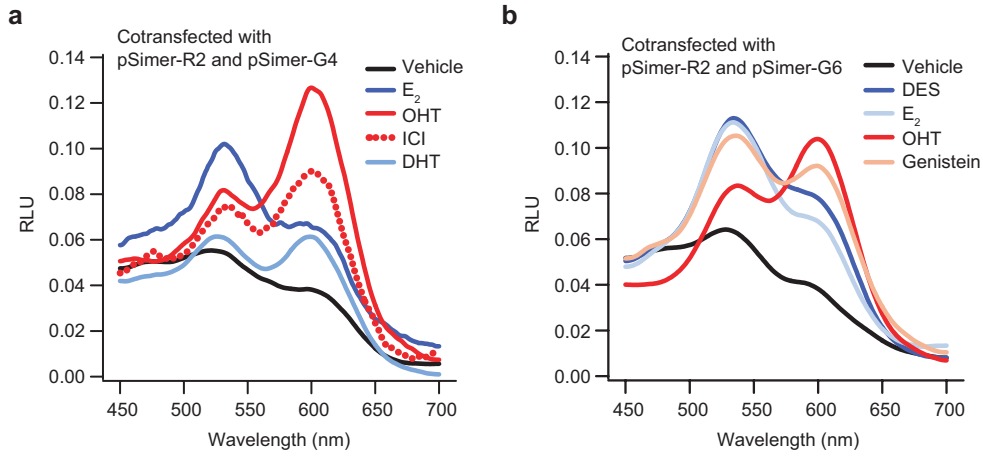

Figure 4. a) Luminescence spectra of COS-7 cells carrying pSimer-R2 and pSimer-G4 in response to various ligands. These spectra enable us to score agonistic and antagonistic activities of a ligand on the basis of luminescence intensity variances (Δ LI) at 540 and 610 nm. The scores are specified in Supplementary Table 1. b) Luminescence spectra of COS-7 cells carrying pSimer-R2 and pSimer-G6 in response to various ligands. This represents a method of simultaneously scoring agonistic and antagonistic activities of a ligand on the basis of luminescence intensity variances (ΔLI) at 540 and 610 nm. The scores are specified in Supplementary Table 2.

Simultaneous Determination of Agonistic and Antagonistic Activities of a Ligand for ER with a Luminescence Strip Carrying Dried Luminescent Probes. Agonistic and antagonistic activities of a ligand for ER were examined with a cross-like luminescence strip carrying dried luminescent probes (Figure 6, panels a and b). After inlet of a substrate solution carrying E_2 or OHT in the middle of the cross-section, the increase of luminescence intensities at the end circles of the crosses were monitored. The cross end mounted with a lysate of intact COS-7 cells (area 1; Figure 6, panel a) exhibited only a background luminescence in response to 10^{-5} M of E_2 or OHT, whereas the other ends of the cross were illuminated in response to the ligands. The cross end mounted with the red-light-emitting probe from pSimer-R2 sensitively varied its light in response to OHT (area 2). On the other hand, the cross end with green-light-emitting probe from pSimer-G6 was selectively illuminated in response to E_2 (area 3). Meanwhile, the cross end with the probe from pSimer-RG2 emitted strong light in response to both ligand stimulations (area 4). The luminescence spectra shown in Figure 5, panel a suggest that the light of area 4 is a characteristic mixture of green and red light, which reflects the genomic and nongenomic activities of a ligand.

DISCUSSION

Bioactive small molecules including steroid hormones exert multiple effects on various signaling pathways inside mammalian cells. For instance, some steroids activate genomic and nongenomic pathways at the same time (*2*), and some of the signaling pathways of steroids crosstalk with others. Unfortunately, any conventional methods cannot illuminate simultaneously such multiple effects of a ligand in living subjects.

Here, we demonstrate a methodology for determining such bifacial effects of a ligand in mammalian cells. We first developed a single-molecule-format probe emitting red luminescence as an index of the activities of estrogen antagonist in a nongenomic signaling pathway mediated by Src. The tyrosine phosphorylation recognition domain SH2 of Src, a well-known target for anticancer studies (*18*), was fused to ER LBD. The Src SH2-fused ER LBD was sandwiched with N- and C-terminal

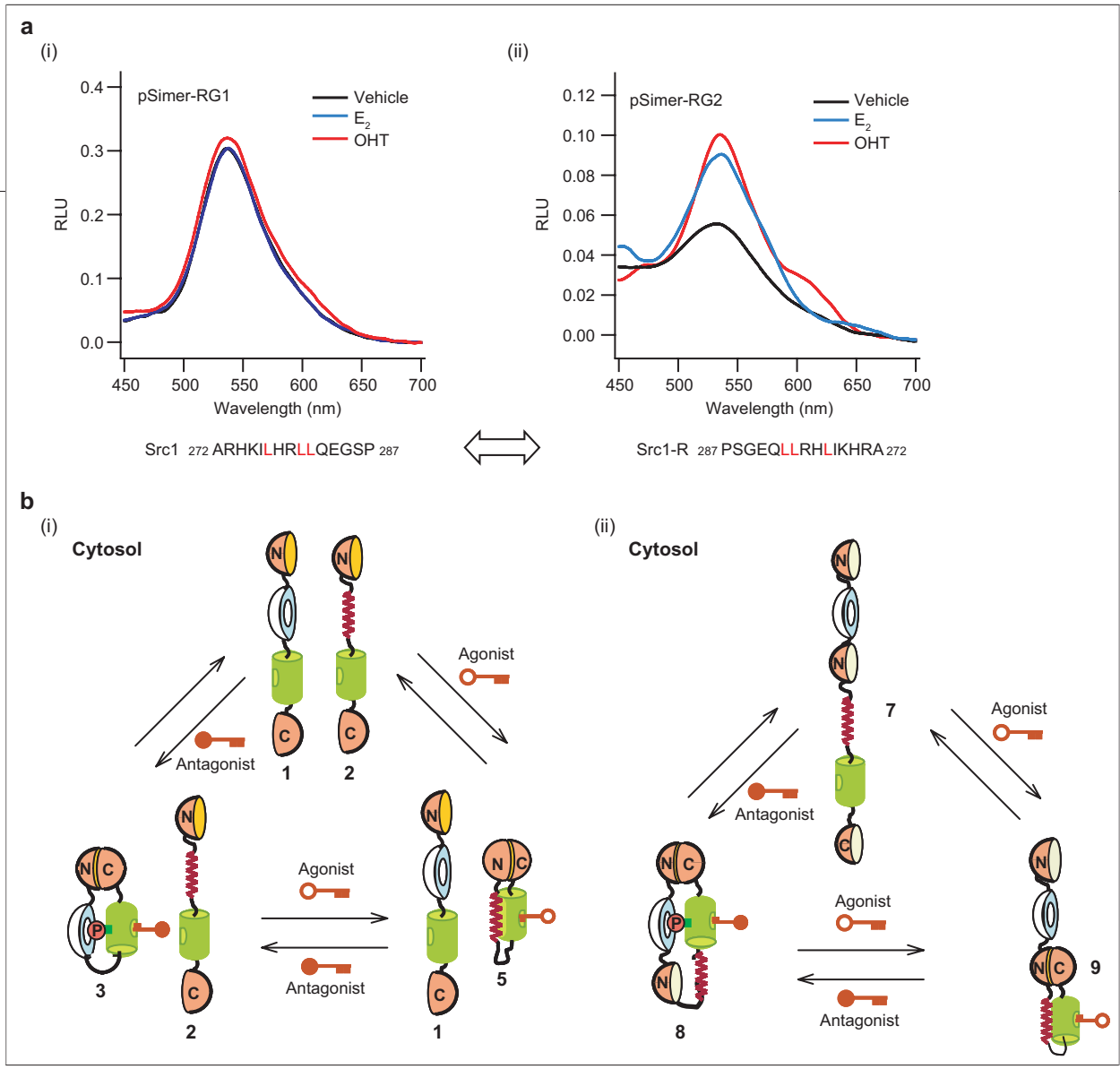

Figure 5. a) Luminescence spectra of COS-7 cells carrying pSimer-RG1 (i) or pSimer-RG2 (ii) in response to a ligand. b) Illustrative diagram of intramolecular folding of multicolor probes in response to ligands. (i) Molecular structures of each probe in response to agonist and antagonist in a cell carrying both pSimer-R and -G series probes. (ii) Molecular structures of the probe in response to agonist and antagonist in a cell carrying a pSimer-RG series probe.

fragments of CB Red. From the viewpoint that phosphorylation of proteins is a major means for endogenous signaling transduction in live cells (*19, 20*), the present single-molecule-format probe provides a unique and powerful strategy for recognizing protein phosphorylation through illuminating the signal transductions inside living cells. This is the first example where phosphorylation is recognized with a bioluminescent probe.

As an optimal luciferase for this probe, we took advantage of click beetle luciferase (CB). CB is especially less sensitive to pH, temperature, and heavy metals and emits a stable light with D-luciferin in physiological circumstances (*5, 11*). The optimal dissection point for this probe was found to be between 412 and 413 aa of CB Red (Figure 2, panel a). However, our previous study revealed that fragments dissected between 439 and 440 aa of CB Red exhibited the best signal-to-background ratio for the single-molecule-format probe for AR LBD-LXXLL motif binding (*11*). These two results conclude that each single-molecule-format probe requires its own optimal dissection sites of CBs to exhibit a favorable recovery of luciferase activity. Two factors should be considered for this optimal complementation of CB fragments: (i) steric hindrance among the components during the intramolecular complementation of the split CB fragments and (ii) a special mismach between the fragments. If one of the component proteins of the probe has a too short or too long arm, a special mismatch between the flanked N- and C-terminal fragments can oc-

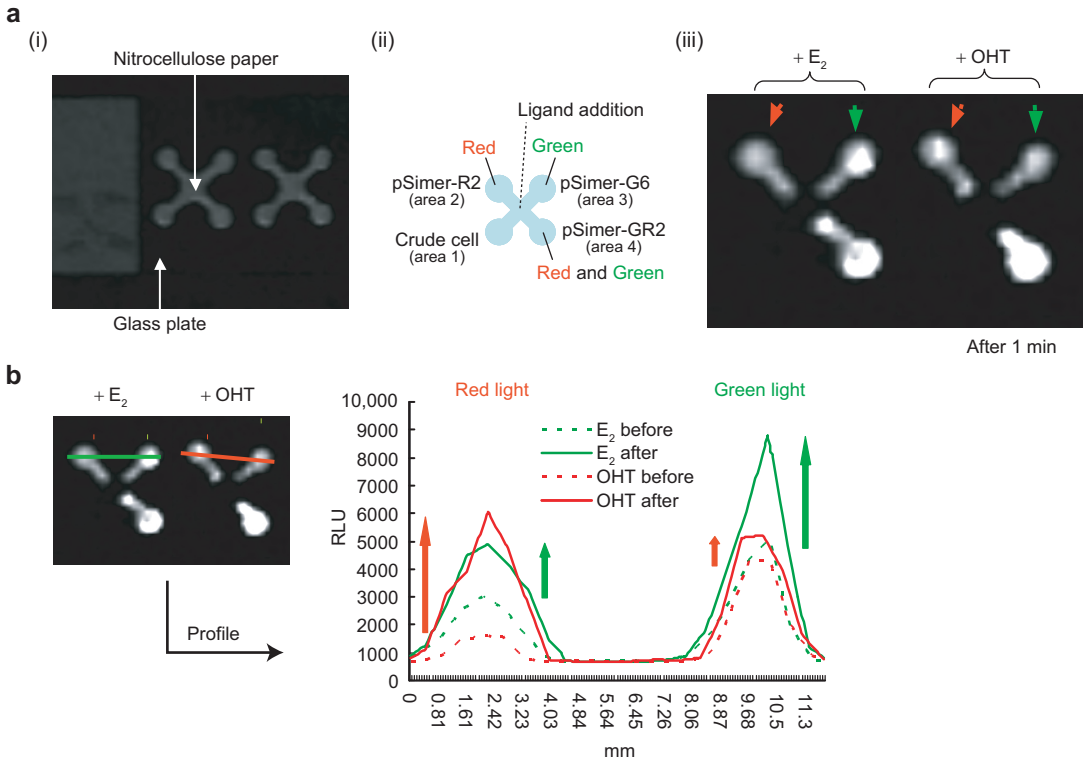

Figure 6. a) Estimation of agonistic and antagonistic activities of a ligand using a luminescence strip carrying dried bioluminescent probes. (i) Picture of the luminescence strip. (ii) Map of the probes deposited on the strip. (iii) Representative image of the red and green luminescence emitted from the strip in response to E_2 or OHT. A substrate solution with a ligand was applied in the middle of the strip as marked with a dot line in (ii). b) The profile of the red and green luminescence from the strip before and after injection of E_2 or OHT. Red light was highly increased upon sensing OHT, whereas green light was enforced by E_2.

cur. This might cause variances in the optimal dissection points of CB for determining protein−protein interactions inside a single-molecule-format probe.

According to an X-ray crystallography study for FLuc, FLuc consists of a globular N-terminal region (1−435 aa) and a compact C-terminal domain (441−550 aa). They are linked with a flexible loop region (436−440 aa) (*29*). Although crystallographic data of CB were not reported, the structure of CB is almost the same as that of FLuc from the viewpoint of the following homology factors between CB and FLuc: (i) they are both members of a superfamily of acyl-adenylate-forming enzymes, and (ii) the two hydrophobicity diagrams of the amino acids based on the scale of Kyte et al. (*30*) are almost superimposable. Considering all this, we conclude that the effective dissection points of CB should be inside or near the flexible loop region between 380 and 480 aa of CB for constructing an efficient single-molecule-format bioluminescent probe. Inside the single-molecule-format probe, split CB undergoes a temporal loss of enzyme activity. Upon ligand stimulation, the activities are recovered through a complementation of the N- and C-terminal fragments of CB.

The luminescence intensities from COS-7 cells carrying pSimer-R2 reached a plateau at 15 min after addition of 10^{-5} M OHT (Figure 2, panel c), which indicates that the probe takes 15 min to complete all of the steps for recovering luciferase activities. This response time comprises all the periods for (i) plasma membrane penetration of OHT, (ii) ER LBD-OHT binding, (iii) conformational change and phosphorylation (Tyr537) of ER LBD, (iv) ER LBD-Src SH2 binding, and (v) a subsequent protein complementation between the flanking N- and C-terminal fragments of CBs, at both ends of the fusion

protein ER LBD-Src SH2. It is beneficial to consider the rate-determining step among the periods. Surface plasmon resonance studies previously demonstrated that E_2-ER binding (step 2) and the subsequent ER-coactivator approximation (steps 3 and 4) are completed in less than 10 s (*12*) and in just a few minutes (*22*), respectively. It was also discussed that protein complex assembly (complementation; step 5) and disassembly are completed typically within a few minutes (*11, 23*). Thus, these steps are unlikely to be a rate-determining step.

The molecular structure of the present single-molecule-format probe is very similar to that of a conventional FRET probe. Therefore, the comparison is beneficial for understanding the ligand-sensing kinetices of ER. It was previously reported that fluorescence intensities by FRET reached a plateau in 13 min in the case of ER LBD-LXXLL motif binding and 20 min in the case of AR LBD-LXXLL motif binding (*7, 24*). Another group also reported that at least 20 min is required to reach a plateau of fluorescence from a FRET probe comprising full-length AR (*8*). These cases using FRET require a similar time as the present method to reach a plateau of fluorescence. It is notable that FRET, different from the present probe, does not require step 5 for signal development. This comparison between FRET and the present method suggests that the rate-determining step in the present probe system is the plasma membrane permeation of ligands (step 1). This observation is also supported by a previous time-course study using a radioisotope, where 10 min is consumed for the 90% uptake of an endogenous steroid by the plasma membrane (*25*). It is considered that although steroids are small hydrophobic drugs, they commonly comprise hydrophilic side chains such as hydroxyl and/or carboxy groups. Their penetration over the plasma membrane appeared to be consequently retarded.

The roles of Tyr537 in the ligand-sensitivity of human ER (hER) have been intensively studied previously (*15, 26, 27*). The phosphorylation of tyr537 is a prerequisite of pivotal actions of ER including (i) estrogen-dependent hyperphosphorylation of the serine residues, (ii) dimerization, (iii) nuclear retention, and (iv) DNA binding (*15, 28*). A mutated form, Y537N, was isolated from a patient having metastatic tamoxifen-resistant breast cancer (*28*). The phosphorylation mechanism of ER at Tyr537 in the nongenomic pathways is vague and argued about among researchers. Arnold et al. reported that (i) phosphorylation of Tyr537 of hER is regulated by *c*-Src and occurs independent of estrogen and (ii) the phosphorylation of Tyr537 increases estradiol-binding capacity (*15, 27*). On the other hand, Migliaccio et al. demonstrated that E_2-bound ER stimulates the Src/Ras/Erk pathway of cancer cell lines (*26*). These previous studies suggest that (i) E_2-ER binding may activate various tyrosine kinases via a nongenomic pathway; (ii) *c*-Src, one of the kinases, phosphorylates Tyr537 of ER; and (iii) subsequently E_2-binding capacity of ER is enhanced. On the basis of this consideration, we designed a single-molecule-format probe with Src SH2-fused ER LBD for recognizing protein phosphorylation. The probe was more sensitive to OHT than to cyproterone acetate (CPA), although both OHT and CPA are estrogen antagonists exhibiting similar inhibitory effects to genomic actions of ER. Our mutagenesis study proved that this ER LBD-Src SH2 domain binding is mediated by the phosphorylation of Tyr537 of ER LBD. In contrast, E_2 weakly contributed to ER LBD-Src SH2 domain binding considering that the luminescence intensities were only twice as high as the basal intensities. It is of interest that the present probe is sensitive only to antagonists and not to agonists. This result indicates that the antagonist-induced ER LBD-Src SH2 binding is more favorable for the subsequent complementation between the flanked N- and C-terminal fragments of CB than the agonist-stimulated one.

According to the Western blot analysis (Figure 2, panel e), both OHT and E_2 phosphorylate ER at Y537 to a similar extent. Nevertheless, we observed that OHT triggers much stronger luminescence intensities from SIMER-R2 than E_2, which is similar to a result reported by Gambhir et al. with an intramolecular folding sensor using ER LBD and split-*Renilla* luciferase (*6*). The present results should be interpreted with the molecular conformation of ER LBD, rather than with the degree of ER phosphorylation. There is no doubt that the luminescence intensities reflect the hormonal activities of OHT and E_2. Although both OHT and E_2 phosphorylate ER at Y537 to the same extent, the conformation changes of ER differ. Y537 is in the hinge region of helix12 of ER, the orientation of which is dramatically changed according to the property of ligands. The conformation of ER modulated by OHT is considered to be more appropriate for recruiting Src SH2 than that by E_2. This appeared in the enhanced luminescence intensities by OHT.

The collected evidence in Figure 2, panels a−e and Supplementary Figure 1 supports the following conclusions: (i) OHT, not E_2, efficiently induces the appropriate conformational change of ER LBD and the subsequent ER LBD-Src SH2 binding via a phosphorylation of Tyr537 of ER LBD; (ii) this probe emits specific red light with a single peak at 610 nm reporting nongenomic activities of estrogen antagonists, OHT, and ICI 182780; (iii) endogenous tyrosine kinases stimulated by EGF do not cross-activate phosphorylation of ER LBD; (iv) this probe provides a useful measure for determining protein phosphorylation and subsequent protein−protein interactions, which occur within a short time (several minutes) inside mammalian cells; and (v) this ER LBD-Src SH2 binding is useful for estimating ligand activities in the nongenomic pathway of ER mediated by Src considering the interaction of ER with Src is a typical pathway of nongenomic steroid signaling through ER.

Conventionally, agonist and antagonist have been defined according to their genomic activities. However, this conventional definition is not always correct for explaining the activities of a ligand in nongenomic signaling pathways. In this study, OHT, an antagonist for genomic signaling pathways of ER, was unexpectedly a strong agonist for AR-Src binding known as a nongenomic signaling pathway.

Reversibility of a bioluminescent probe is an attractive issue for evaluating the sensorial performance. The present experiment revealed that SIMER-G6, which comprises ER LBD, is irreversible after binding E_2 (Figure 3, panel b(iii)). On the contrary, previous single-molecule-format probes with AR LBD were interestingly reversible after binding DHT (*11, 12*). We believe that these two results should be interpreted as follows: it should be noted that ER and AR fundamentally differ in the physiological life span. Agonist-activated AR is recycled after transcription activation, whereas agonist-bound ER is decomposed after transcription (*31*). This means that deprivation of a ligand from ER is a useless step in physiological circumstances. This intrinsic difference between AR and ER may appear the consequences.

The present probe system provides a new methodology for visualizing bifacial, multiple activities of a ligand with green or red lights. The probe system exhibited characteristic bioluminescent spectra with bands at ~540 nm (green) and ~610 nm (red) in response to each ligand. The bifacial activities of a ligand should be normalized for a comparison with those of others. However, no appropriate method was suggested to normalize multiple activities of a ligand. Here, we propose a method to relatively score agonistic and antagonistic activities of a ligand (named ES), where ES is defined as the increase in bioluminescence intensity at 540 nm divided by that at 610 nm (DRLU540/DRLU610). Through this ES value, we can easily categorize ligands in agonistic, antagonistic, and neutral groups and compare the bifacial activities of a ligand with the score.

Cell-based bioanalytical methods are categorized into (i) genetic, transcriptional and (ii) nontranscriptional assays. A genetic, transcriptional assay such as a reporter gene assay requires a long ligand stimulation time until sufficient accumulation of a reporter protein is reached. The present method is characterized as a nontranscriptional assay using an intracellular complementation, which is beforehand expressed and localized in adequate intracellular compartments of interest. The luminescence intensity is ready to be developed upon the cell being stimulated by a signal. The present data acquisition time, 15 min, is largely shortened in comparison with that of the protein-splicing schemes, which require at least 2 h (*4, 32*). Thus, the present method is applicable to a high-throughput analysis of the activities of bioactive small molecules, which activate temporal, short-time molecular events.

In the present study, we examined two types of multicolor system: one is a probe set with two single-molecule-format probes independently emitting red and green light; the other is a single-molecule-format multicolor probe comprising all the components for emitting red and green light in a single molecule. The equilibrium diagrams for both cases are illustrated in Figure 5, panel b. The spectra in Figure 5, panel a(ii) show that the single-molecule-format multicolor system emits a considerable green light even in the absence of any ligand. The results demonstrate that (i) the basal interactions between ER LBD and the LXXLL motif occur even in the absence of a ligand, which caused the high background luminescence intensities at 540 nm and that (ii) ER LBD inside SIMER-RG2 recognizes the adjacent LXXLL motif and/or SH2 domain with a certain ratio in response to E_2 or OHT, whose spectral pattern reflects bifacial activities of each ligand.

To demonstrate the advantage of the present probe in practical on-site analysis, the probes were immobi-

lized in each end of a cross-like nitrocellulose strip and examined bifacial activities of a ligand (Figure 6). It is important to know whether multiple activities of a ligand can be evaluated even with a portable, on-site sensor strip. It is a very promising result for further applications that each end of the cross-like sensor strip exhibited characteristic colors in response to E_2 or OHT.

We mounted 5 μL of the cell lysates on each cross end of the strip. The area of the circular ends of the cross end is 6.8 mm^2, on which 0.87 μg of the total proteins was mounted. The total amount of proteins in 5 μL of the cell lysates was determined with a Bradford reagent. Because ~0.01% of the total amount of proteins was of the luminescent probe, ca. 0.84 fmol of the probe emitting red light was mounted on the cross end of the strip. The results show that (i) this sensor strip enables an on-site determination of ligand activities and (ii) ca. 0.84 fmol of the probe emitting red or green light on a strip is enough for evaluating ligand activities.

Taken together, we developed multicolor systems for illuminating bifacial effects of a target ligand in mammalian cells: a multicolor probe set and a single-molecule-format multicolor probe. The multicolor systems exhibited characteristic green and/or red lights in response to a ligand. Luminescence intensity spectra with bands at 540 and 610 nm were recorded to simultaneously determine the bifacial activities of a ligand. These results demonstrate that the present strategy using multiple fragments of split CB Red and CB Green is feasible for determining bifacial activities of ligands via intramolecular protein−protein (peptide) interactions of interest. Although we exemplified a two-color probing system with ERa, multiple signal transductions could be imaged with the same scheme shown in this study.

METHODS

Construction of Plasmids. As templates for PCR, pCBG99-Control and pCBR-Control were obtained from Promega. The constructs of pSimer-R series plasmids were made according to the following steps. The cDNAs of N- and C-terminal fragments of CB Red and Green were generated by PCR to introduce unique restriction sites, *Hin*dIII/*Kpn*I or *Bam*HI/*Xho*I at both ends of the fragments using adequate primers and the template vector. The dissected five pairs of the N- and C-terminal fragments were as follows: (i) 1−439 aa and 440−542 aa, (ii) 1−412 aa and 413−542 aa, (iii) 1−442 aa and 443−542 aa, (iv) 1−439 aa and 443−542 aa, and (v) 1−439 aa and 437−542 aa. Meanwhile, the cDNAs encoding ER LBD (305−550 aa) and Src SH2 (150−248 aa) were synthesized by PCR to add adequate restriction sites, *Nhe*I/*Bam*HI and *Kpn*I/*Nhe*I (*Not*I), respectively, at both ends. The PCR-amplified cDNA fragments were then subcloned in the corresponding restriction enzyme-digested pcDNA 3.1(+) vector backbone. They were named pSimer-R1 to -R5 according to the position of dissection sites in CB Red. The expressed fusions may be called SIMER-R1 to -R5.

On the other hand, the constructs for pSimer-G series plasmids were made according to the following steps. The cDNAs of N- and C-terminal fragments of CB Green were generated by PCR to introduce unique restriction sites, *Not*I/*Eco*RI and *Bam*HI/*Xho*I, respectively, at both ends of the fragments using adequate primers and the template vector. The cDNAs encoding ER LBD and Src SH2 were synthesized by PCR to add adequate restriction sites, *Nhe*I/*Bam*HI and *Eco*RI/*Nhe*I, respectively, at both ends. The PCR-amplified cDNA fragments were then subcloned in the pcDNA 3.1(+) vector (Invitrogen) backbone that was digested with the corresponding restriction enzymes. They were named pSimer-G1 to -G6, in which the LXXLL motif differs. The information about amino acid sequence consisting of the LXXLL motifs in the ER coactivators, Rip140 and Src1, were taken from GenBank and the first paper described the original interests of LXXLL motifs (*17*). The specific sequences were as follows: pSimer-G1, ^{685}ARHKI**L**HR**LL**QEGSP^{699} (the fourth LXXLL motif of SRC1); pSimer-G2, ^{699}PSGEQ**LL**RH**L**IKHRA^{685} (the reverse fourth LXXLL motif of SRC1); pSimer-G3, ^{495}HQKVT**L**LQ**LL**LGHKN^{509} (the sixth LXXLL motif of Rip140); pSimer-G4, ^{509}NKHGL**LL**QL**L**TVKQH^{495} (the reverse the sixth LXXLL motif of Rip140); pSimer-G5, ^{932}SFNV**L**KQ**LL**LSENCV^{946} (the ninth LXXLL motif of Rip140); and pSimer-G6, ^{946}VCNESL**LL**QK**L**VNFS^{932} (the reverse ninth LXXLL motif of Rip140). The expressed fusions may be called SIMER-G1 to -G6. The word "reverse" in the parenthesis means the consequent folding nature after binding.

The constructs for pSimer-RG series plasmids were made according to the following steps: The cDNA construct of pSimer-RG2 was assembled on the basis of the backbone of pSimer-G6 and -R2 as shown in Figure 1, panel b. On the other hand, The construct of pSimer-RG1 were assembled on the basis of the backbone of pSimer-G5 and -R2. The cDNA fragment encoding the N-terminal fragment of CB Green and LXXLL motif were ligated between *Not*I and *Nhe*I of a pSimer-R2 backbone. pSimer-RG3 comprises the same construct as pSimer-RG2 except for the GS linker length between LXXLL motif and ER LBD: pSimer-RG2 has 10 GS linker, but pSimer-RG3 contains 20 GS linker. They were named pSimer-RG1 and -RG3. The expressed fusions may be called SIMER-RG1 to -RG3.

The *E. coli* strain DH5α was used as the bacterial host for all plasmid constructions. All DNA sequences of the plasmids were verified by sequencing with a genetic analyzer ABI PRISM 310 (Applied Biosystems, Tokyo, Japan).

Determination of Ligand Sensitivity of Cells Carrying Each Plasmid. The ligand sensitivities of mammalian cells carrying each constructed plasmid were estimated as follows. One of the plasmids was introduced into the following mammalian cells, HeLa, COS-7, NIH 3T3, or MCF-7, using *Trans*IT-LT1 (0.5 μg of plasmid for each well of a 24-well plate). The cells carrying each plasmid were incubated in a 5% CO_2 incubator for 16 h. The cells on the 24-well plate were stimulated with a specific ligand or vehicle (0.1% v/v DMSO) for 20 min. The luminescence intensities by each probe expressed in each cell line on the 24-well plate were then developed using a Bright-Glo substrate solution (Promega). The brief procedure for the Bright-Glo substrate solution was as follows. The cells on the 24-well plate were washed once with PBS. A 40 μL lysate of substrate solution prepared according to the manufacturer's instruction was added to each

well of the plates. After incubation for 3 min at 37 °C, the developed luminescence intensities from the cell lysates were recorded with a luminometer (Minilumat LB9506; Berthold). The luminometer provides the luminescence intensities with a relative luminescence unit (RLU) because the photons are multiplied in the light-detecting unit of the luminometer. The data in Figure 2, panels a(i) and a(iii); Figure 3, panel a(iii); Figure 4, panels a and b; and Figure 5, panel a were expressed with RLU clarifying the direct luminescence intensities from the luminometer. On the other hand, the data in Figures 2, panels b–d and Figure 3, panels a(i) and b were shown with RLUs normalized to the amount of proteins. For this normalization, the amounts of proteins were sequentially determined using a protein assay kit (Bio-Rad) after the measurements of luminescence intensity. The luminescence normalized against the amount of proteins was expressed as "RLU/μg protein," which means the luminescence intensity per 1 μg of proteins. "RLU ratio (±)" means the luminescence ratio of RLU (+) to RLU (−). RLU (+) and RLU (−) are the RLU per 1 μg protein of the cell lysates treated with a ligand and a vehicle (0.1% (v/v) DMSO), respectively.

Western Blotting. Phosphorylation of SIMER-R2 and -R2m was examined with a Western blot analysis (Figure 2, panel e). COS-7 cells carrying pSimer-R2 or pSimer-R2m were cultured in a 6-well plate. The cells were stimulated with vehicle (0.1% v/v DMSO), 10^{-6} M E_2, or 10^{-6} M OHT for 30 min. The cells were washed with PBS, lysed in 200 μL of lysis buffer (1% (w/v) SDS, 10% (v/v) glycerol, 10% (v/v) 2-mercaptoethanol, 0.001% (w/v) Bromophenol Blue, 50 mM Tris-HCl, pH 6.8), and boiled in 95 °C for 5 min. Each 7 μL sample was electrophoresed in a 10% (w/v) polyacrylamide gel, transferred to a nitrocellulose membrane, and blotted with a rabbit anti-ER Y537 antibody (Santa Cruz) or a mouse anti-β-actin antibody (Sigma). Lanes 1–3 show the blots from lysates of COS-7 cells carrying pSimer-R2, whereas lanes 4–6 present the blots from lysates of COS-7 cells carrying pSimer-R2m.

Monitoring Spectra of Luminescence Intensities Triggered by Each Ligand. The spectra shown in Figure 2, panel a(iii); Figure 3, panel a(iii); Figure 4, panels a and b; and Figure 5, panel a were taken on the basis of the following protocol. COS-7 cells were raised in a 6-well plate to 90% confluence. The cells on each well were transiently transfected with 2.5 μg of a plasmid or a mixture of plasmids. Sixteen hours after the transfection, the cells were stimulated with each ligand for 20 min. An aliquot of Bright-Glo substrate solution (400 μL) was then added to each well of the 6-well plate and incubated for another 3 min. Luminescence spectra from the reconstituted luciferase were recorded with a spectrometer (FP-750; Jasco). The vertical axes were expressed with an arbitrary unit (AU) per wavelength (nm).

Ligand-Dependent Kinetics in Luminescence Intensities by pSimer-R2. Kinetics of the luminescence intensities triggered by ligands was monitored with the COS-7 cells carrying pSimer-R2 (Figure 2, panel c). The COS-7 cells were cultured in 12-well plates, transiently transfected with pSimer-R2, and then incubated for 16 h before stimulations. At 0, 5, 10, 15, 20, and 25 min after addition of E_2 or OHT, the luminescent intensities were estimated using a Bright-Glo substrate kit and a luminometer Minilumat LB9506.

Dose–Response Curves for Ligands. Luminescence intensities correlated with a dose of ligands were determined using COS-7 cells carrying pSimer-G4 or -G6 (Figure 3, panel b). COS-7 cells cultured in 24-well plates were transiently transfected with pSimer-G4 or -G6. After 16 h of incubation, the cells were stimulated for 20 min with varying concentrations of DHT, OHT, or E_2. Finally, we estimated the luminescence intensities of each well that was developed using the Bright-Glo substrate solution.

Reversibility of SIMER-G6. The reversibility of SIMER-G6 to E_2 was examined (Figure 3, panel b(iii)). COS-7 cells carrying pSimer-G6 were raised in a 24-well plate and stimulated with vehicle (0.1% (v/v) DMSO) or E_2 for 20 min. The culture medium was then replaced with a fresh one for eliminating E_2, and the subsequent variance of luminescence intensities was monitored every 20 min.

Construction of Bioluminescence Strip for Estimating Multiple Activities of a Ligand *in Vitro*. An *in vitro* study was performed with a bioluminescence strip carrying the optimal probes emitting red and/or green light in response to a ligand (Figure 6, panels a and b).

A nitrocellulose paper was utilized for mounting a cross-like sensor strip on a glass slide. A cross-like strip (1.1 × 1.1 cm) was clipped from a sheet of nitrocellulose paper and glued on a glass slide (2 × 7 cm).

COS-7 cells were transiently transfected with pSimer-R2, pSimer-G6, or pSimer-RG2 and incubated for 16 h in a 5% CO_2 incubator. The cells on a 12-well plate were washed once with PBS and additionally incubated in the incubator for 3 min after addition of an 80 μL of lysis buffer provided from the Bright-Glo assay kit. Each 5 μL of the cell lysates obtained from the COS-7 cells carrying pSimer-R2, pSimer-G6, or pSimer-RG2 were mounted on each end circle (area 6.8 mm^2) of the cross-like strip made of nitrocellulose paper and dried for 5 min in a 37 °C dry oven. The background luminescence from the strips was recorded with a luminescence scanner (RAS-3000, FujiFilm) before determination of ligand activities. A 10 μL substrate solution supplemented with 10^{-5} M E_2 or 10^{-5} M OHT (final concentration) was dropped in the middle of the strip (cross-section), and the subsequent luminescence intensities at each end circle of the cross were integrated with the scanner for 1 min.

Mammalian Two-Hybrid Assay. A mammalian two-hybrid assay was conducted for cross-checking ER LBD—LXXLL motif binding (Supplementary Figure 2). The cDNA construct of pSimer-G6 was fragmented in two parts. Each fragment was fused to cDNAs of Gal4 and VP16, respectively. The new constructs comprising LXXLL motif and ER LBD were subcloned into pACT and pBIND vectors (Promega), respectively, and named pACT-LXX and pBIND-ER. COS-7 cells raised in a 24-well plate were cotransfected with pACT-LXX, pBIND-ER in addition to pG5luc (Promega). The cells were incubated for 24 h and stimulated with vehicle (0.1% (v/v) DMSO), 10^{-6} M OHT, or 10^{-6} M E_2. Twenty-four hours after stimulation, the cells were harvested, and the subsequent luminescence intensities were developed with the specific substrate solution (Bright-Glo, Promega).

Supporting Information Available: This material is available free of charge *via* the Internet.

REFERENCES

1. Aggarwal, B. B. (2003) Signalling pathways of the TNF superfamily: a double-edged sword, *Nat. Rev. Immunol. 3*, 745–756.
2. Kim, S. B., Kanno, A., Ozawa, T., Tao, H., and Umezawa, Y. (2007) Nongenomic activity of ligands in the association of androgen receptor with Src, *ACS Chem. Biol. 2*, 484–492.
3. Paulmurugan, R., Umezawa, Y., and Gambhir, S. S. (2002) Noninvasive imaging of protein-protein interactions in living subjects by using reporter protein complementation and reconstitution strategies, *Proc. Natl. Acad. Sci. U.S.A. 99*, 15608–15613.
4. Kim, S. B., Ozawa, T., Watanabe, S., and Umezawa, Y. (2004) High-throughput sensing and noninvasive imaging of protein nuclear transport by using reconstitution of split Renilla luciferase, *Proc. Natl. Acad. Sci. U. S. A. 101*, 11542–11547.
5. Viviani, V. R., Uchida, A., Viviani, W., and Ohmiya, Y. (2002) The influence of Ala243 (Gly247), Arg215 and Thr226 (Asn230) on the bioluminescence spectra and pH-sensitivity of railroad worm, click beetle and firefly luciferases, *Photochem. Photobiol. 76*, 538–544.

6. Paulmurugan, R., and Gambhir, S. S. (2006) An intramolecular folding sensor for imaging estrogen receptor-ligand interactions, *Proc. Natl. Acad. Sci. U.S.A. 103*, 15883–15888.
7. Awais, M., Sato, M., Lee, X. F., and Umezawa, Y. (2006) A fluorescent indicator to visualize activities of the androgen receptor ligands in single living cells, *Angew. Chem., Int. Ed. 45*, 2707–2712.
8. Schaufele, F., Carbonell, X., Guerbadot, M., Borngraeber, S., Chapman, M. S., Ma, A. A. K., Miner, J. N., and Diamond, M. I. (2005) The structural basis of androgen receptor activation: Intramolecular and intermolecular amino-carboxy interactions, *Proc. Natl. Acad. Sci. U.S.A. 102*, 9802–9807.
9. Sato, M., Hida, N., Ozawa, T., and Umezawa, Y. (2000) Fluorescent indicators for cyclic GMP based on cyclic GMP-dependent protein kinase Iα and green fluorescent proteins, *Anal. Chem. 72*, 5918–5924.
10. Paulmurugan, R., and Gambhir, S. S. (2005) Firefly luciferase enzyme fragment complementation for imaging in cells and living animals, *Anal. Chem. 77*, 1295–1302.
11. Kim, S. B., Otani, Y., Umezawa, Y., and Tao, H. (2007) Bioluminescent indicator for determining protein-protein interactions using intramolecular complementation of split click beetle luciferase, *Anal. Chem. 79*, 4820–4826.
12. Kim, S. B., Awais, M., Sato, M., Umezawa, Y., and Tao, H. (2007) Integrated molecule-format bioluminescent probe for visualizing androgenicity of ligands based on the intramolecular association of androgen receptor with its recognition peptide, *Anal. Chem. 79*, 1874–1880.
13. Evans, R. M. (1988) The steroid and thyroid hormone receptor superfamily, *Science 240*, 889–895.
14. Bjornstrom, L., and Sjoberg, M. (2005) Mechanisms of estrogen receptor signaling: convergence of genomic and nongenomic actions on target genes, *Mol. Endocrinol. 19*, 833–842.
15. Arnold, S. F., Vorojeikina, D. P., and Notides, A. C. (1995) Phosphorylation of tyrosine 537 on the human estrogen receptor is required for binding to an estrogen response element, *J. Biol. Chem. 270*, 30205–30212.
16. Shiau, A. K., Barstad, D., Loria, P. M., Cheng, L., Kushner, P. J., Agard, D. A., and Greene, G. L. (1998) The structural basis of estrogen receptor/coactivator recognition and the antagonism of this interaction by tamoxifen, *Cell 95*, 927–937.
17. Heery, D. M., Kalkhoven, E., Hoare, S., and Parker, M. G. (1997) A signature motif in transcriptional co-activators mediates binding to nuclear receptors, *Nature 387*, 733–736.
18. Playford, M. P., and Schaller, M. D. (2004) The interplay between Src and integrins in normal and tumor biology, *Oncogene 23*, 7928–7946.
19. Kim, S. B., Takao, R., Ozawa, T., and Umezawa, Y. (2005) Quantitative determination of protein nuclear transport induced by phosphorylation or by proteolysis, *Anal. Chem. 77*, 6928–6934.
20. Lee, S. J., Sekimoto, T., Yamashita, E., Nagoshi, E., Nakagawa, A., Imamoto, N., Yoshimura, M., Sakai, H., Chong, K. T., Tsukihara, T., and Yoneda, Y. (2003) The structure of importin-β bound to SREBP-2: nuclear import of a transcription factor, *Science 302*, 1571–1575.
21. Rich, R. L., Hoth, L. R., Geoghegan, K. F., Brown, T. A., LeMotte, P. K., Simons, S. P., Hensley, P., and Myszka, D. G. (2002) Kinetic analysis of estrogen receptor/ligand interactions, *Proc. Natl. Acad. Sci. U.S.A. 99*, 8562–8567.
22. Suen, C. S., Berrodin, T. J., Mastroeni, R., Cheskis, B. J., Lyttle, C. R., and Frail, D. E. (1998) A transcriptional coactivator, steroid receptor coactivator-3, selectively augments steroid receptor transcriptional activity, *J. Biol. Chem. 273*, 27645–27653.
23. Stefan, E., Aquin, S., Berger, N., Landry, C. R., Nyfeler, B., Bouvier, M., and Michnick, S. W. (2007) Quantification of dynamic protein complexes using Renilla luciferase fragment complementation applied to protein kinase A activities in vivo, *Proc. Natl. Acad. Sci. U.S.A. 104*, 16916–16921.
24. Awais, M., Sato, M., Sasaki, K., and Umezawa, Y. (2004) A genetically encoded fluorescent indicator capable of discriminating estrogen agonists from antagonists in living cells, *Anal. Chem. 76*, 2181–2186.
25. Strel'chyonok, O. A., and Avvakumov, G. V. (1991) Interaction of human CBG with cell membranes, *J. Steroid Biochem. Mol. Biol. 40*, 795–803.
26. Migliaccio, A., Castoria, G., Di Domenico, M., de Falco, A., Bilancio, A., Lombardi, M., Bottero, D., Varricchio, L., Nanayakkara, M., Rotondi, A., and Auricchio, F. (2002) Sex steroid hormones act as growth factors, *J. Steroid Biochem. Mol. Biol. 83*, 31–35.
27. Arnold, S. F., Melamed, M., Vorojeikina, D. P., Notides, A. C., and Sasson, S. (1997) Estradiol-binding mechanism and binding capacity of the human estrogen receptor is regulated by tyrosine phosphorylation, *Mol. Endocrinol. 11*, 48–53.
28. Zhong, L., and Skafar, D. F. (2002) Mutations of tyrosine 537 in the human estrogen receptor-alpha selectively alter the receptor's affinity for estradiol and the kinetics of the interaction, *Biochemistry 41*, 4209–4217.
29. Conti, E., Franks, N. P., and Brick, P. (1996) Crystal structure of firefly luciferase throws light on a superfamily of adenylate-forming enzymes, *Structure 4*, 287–298.
30. Kyte, J., and Doolittle, R. F. (1982) A simple method for displaying the hydropathic character of a protein, *J. Mol. Biol. 157*, 105–132.
31. Tyagi, R. K., Lavrovsky, Y., Ahn, S. C., Song, C. S., Chatterjee, B., and Roy, A. K. (2000) Dynamics of intracellular movement and nucleocytoplasmic recycling of the ligand-activated androgen receptor in living cells, *Mol. Endocrinol. 14*, 1162–1174.
32. Ozawa, T., Takeuchi, T. M., Kaihara, A., Sato, M., and Umezawa, Y. (2001) Protein splicing-based reconstitution of split green fluorescent protein for monitoring protein-protein interactions in bacteria: improved sensitivity and reduced screening time, *Anal. Chem. 73*, 5866–5874.